Title

An Improved Shape Reconstruction Methodology for Long Rod Like Structures Using Cosserat Kinematics- Including the Poisson's Effect

Permalink

https://escholarship.org/uc/item/73p80625

ISBN

978-3-319-74279-3

Authors

Chadha, Mayank
Todd, Michael D

Publication Date

2019

DOI

10.1007/978-3-319-74280-9_25

Peer reviewed

An improved shape reconstruction methodology for long rod like structures using Cosserat kinematics- including the Poisson's effect

Mayank Chadha[1], Michael D. Todd[2]

Department of Structural Engineering, University of California San Diego, La Jolla, 92093-0085, USA

ABSTRACT: In this paper, we present an improved methodology for the global shape reconstruction of rod-like structures that capture the effect of curvature, shear, torsion, axial deformation, and Poisson's transformation. The inclusion of Poisson's effect relaxes Euler-Bernoulli's rigid cross-section assumption such that the cross-section could now undergo planar deformation (shrinking or expansion in the same plane). This scenario is particularly useful for the inflatable structures and pipelines subjected to large radial pressure.

The theory of shape sensing utilizes the concept of curve framing using Cosserat director triad also called as Cosserat kinematics. The idea is to develop an algorithm to reconstruct the global shape of the rods using the local differential geometry parameters (finite strain parameters) of the midcurve. The deformed configuration of the object lies in $\mathbb{R}^3 \times SO(3) \times \mathbb{R}$ space. The presented theory exploits localized linearization approach that helps to obtain local basis set for the approximation of the midcurve position vector and the director triad, whereas moving least square approximation is utilized to estimate the axial strain field. The uniaxial surface strain incorporating all the effects mentioned above is derived and used to develop the shape-sensing algorithm. A simulation describing the idea is presented at the end.

Keywords: Shape sensing, Cosserat rod theory, Director frame, Local basis function, Scalar surface strain.

1. INTRODUCTION

This paper extends the theory of shape sensing developed by Todd et al. [1] and Chadha and Todd [2-3] to include Poisson's effect along with curvature, shear, torsion and axial deformation. This formulation relaxes Euler-Bernoulli's rigid cross-section. The cross-section remains planar but it can undergo deformation in the plane. The out of plane deformation due to warping is still ignored. Consideration of the Poisson's effect is beneficial in the case of pipes subjected to internal radial pressure or in case of slender inflatable objects.

This theory is geometrical exact and fully nonlinear, so it can capture large deformations. In mathematical terms, this theory involves defining the local differential geometric parameter set (called as "finite strain parameters"), estimating these parameters from the surface strain measurements, and finally using them to reconstruct the deformed configuration (that can be described as differential geometry at large). The configuration of deformable slender objects consists of the beam midcurve framed by the body-centered director triad. The initial description of this type of rod was harnessed by Cosserat and Cosserat [4] to arrive at the finite strain theory of rods and shell. Interested readers may refer to Ericksen and Truesdell [5], Chadha and Todd [6], and the references therein for a brief history and details on this subject.

The subject of shape sensing is a topic of great interest owing to its application in structural health monitoring, smart tethers, and robotic surgical and catheterization applications. Researchers have used various curve framing approaches to capture curvature effects. We maintain a body-centered frame in the unsheared cross-section (as mentioned in Todd et al [1]) and the orthogonal director triad for a general case to capture torsion and shear (as mentioned in Chadha and Todd [2-3]).

As in [1-2], we focus on uniaxial surface strain values obtained from any type of multiplexed sensing approach, including fiber Bragg grating (FBG), Rayleigh backscatter, or conventional resistive strain gauge.

The remainder of the paper is arranged as follows: Section 2 details the geometry of the deformed configuration of the beam and establishes various geometric relationships. Section 3 obtains the expression for uniaxial scalar surface strain including the Poisson's effect. Section 4 describes the solution approach to approximate the deformed configuration. Finally, in section 5, we present a simulation comparing the exact deformed configuration to the predicted results followed by some conclusions.

2. GEOMETRY OF THE DEFORMED CONFIGURATION OF THE BEAM

A rod can be considered as a mathematical object described by a spatial curve in $\mathbb{R}^3$ (the locus of cross-sectional geometric centroid, also called midcurve) parameterized by the arclength $\xi_1 \in \mathbb{R}$, framed by a body-centered Cosserat director triad $\{\mathbf{d}_i(\xi_1)\}$. We consider that the initial unstrained configuration of the beam $\Omega_0 \subset \mathbb{R}^3$ to be straight. Section [2.1] of [2-3] details the geometric description of the beam configuration. The inclusion of Poisson's effect does not change the position vector of the midcurve and the curve framing by the director triad $\{\mathbf{d}_i(\xi_1)\}$; all it changes is the position vector of the material

[1]machadha@ucsd.edu
[2]mdtodd@ucsd.edu

point in the deformed state, which we shall explore further. As a matter of completion, we detail the necessary geometry, in same sense as section [2.1] of [2-3].

Consider a fixed orthogonal frame $\{\mathbf{E_i}\}$. The domain of the beam is defined by the material point $\{\xi_1, \xi_2, \xi_3\}$, such that the origin of the frame $\{\mathbf{E_i}\}$ is at $\{\xi_i = 0\}$ with $i = 1 \dots 3$. Let L_o represent the length of midcurve in the undeformed reference state Ω_o, such that $\xi_1 \in [0, L_o]$. The position vector of any material point in the undeformed configuration Ω_0 is given by $\mathbf{R_0}(\xi_1, \xi_2, \xi_3) = \xi_i \mathbf{E_i}$.

Let us consider that the undeformed (and unstrained) configuration Ω_0 is strained and it deforms to the configuration $\Omega \subset \mathbb{R}^3$. The position vector $\boldsymbol{\varphi}(\xi_1) = \varphi_i \mathbf{E_i}$, represents the midcurve of the deformed configuration. The orientation of any cross-section in the deformed configuration Ω is defined by the set of orthogonal Cosserat director triad $\{\mathbf{d_i}(\xi_1)\}$, such that $\mathbf{d_i}(\xi_1) = d_{ij}(\xi_1)\mathbf{E_j}$. The vector $\mathbf{d_1}(\xi_1)$ is perpendicular to the cross-section and the vectors $\{\mathbf{d_2}(\xi_1), \mathbf{d_3}(\xi_1)\}$ span the cross-section of the beam at ξ_1. Therefore, it may be interpreted that the director field $\{\mathbf{d_i}(\xi_1)\}$ framing the deformed configuration of the beam may be obtained from the fixed frame $\{\mathbf{E_i}\}$ by means of a finite rotation, or

$$\mathbf{d_i}(\xi_1) = \mathbf{Q}(\xi_1)\mathbf{E_i}. \tag{1}$$

Here, $\mathbf{Q}(\xi_1)$ represents family of orthogonal matrices that belongs to $SO(3)$ rotational groups. Hence, they satisfy $\mathbf{QQ^T} = \mathbf{I}$ and $\det \mathbf{Q} = 1$. The orthogonal tensor $\mathbf{Q}(\xi_1)$ is a curve on the manifold $SO(3)$. The tangent vector to this curve in $SO(3)$ is expressed as $\mathbf{Q_{,\xi_1}}$ that represents the tangent space of $SO(3)$. It can be easily obtained that $\mathbf{Q_{,\xi_1}Q^T} = \mathbf{K}(\xi_1)$ such that $\mathbf{K}(\xi_1)$ is the linear space of skew symmetric matrices. Therefore, there exists an axial vector $\boldsymbol{\kappa} = \bar{\kappa}_i \mathbf{d_i}$ associated with $\mathbf{K}(\xi_1)$. Therefore, from (1),

$$\mathbf{d_{i,\xi_1}} = (\mathbf{Q_{,\xi_1}Q^T})\mathbf{d_i} = \mathbf{Kd_i} = \boldsymbol{\kappa} \times \mathbf{d_i}. \tag{2}$$

The vector $\boldsymbol{\kappa} = \bar{\kappa}_i \mathbf{d_i}$ represents the Darboux vector associated with the infinitesimal rotation tensor $\mathbf{K}$, parametrized by ξ_1. Equation (2) represents the differential equation that governs the evolution of the directors and hence the cross-sections.

Let the midcurve $\boldsymbol{\varphi}(\xi_1)$ (parametrized by the undeformed arc-length) be framed by an orthogonal body centered frame $\{\mathbf{T}, \mathbf{V}, \mathbf{H}\}$ such that the vector $\{\mathbf{T}, \mathbf{V}\}$ spans the pitch angle plane and $\mathbf{T}(\xi_1)$ is the tangent vector to the midcurve. Thus, $\mathbf{H} = \mathbf{T} \times \mathbf{V}$. If there is no shearing in the beam, the triad $\{\mathbf{T}, \mathbf{V}, \mathbf{H}\}$ coincides with $\{\mathbf{d_i}\}$. Let $\theta(\xi_1)$ and $\phi(\xi_1)$ represent the pitch and yaw angle of the mid-curve. Therefore, from Fig [4] of Chadha and Todd [6], with $\phi_p(\xi_1) = \theta(\xi_1)$ and $\phi_y(\xi_1) = \phi(\xi_1)$,

$$\begin{bmatrix} \mathbf{T}(\xi_1) \\ \mathbf{V}(\xi_1) \\ \mathbf{H}(\xi_1) \end{bmatrix} = \begin{bmatrix} \cos\theta(\xi_1)\cos\phi(\xi_1) & \sin\theta(\xi_1) & \cos\theta(\xi_1)\sin\phi(\xi_1) \\ -\sin\theta(\xi_1)\cos\phi(\xi_1) & \cos\theta(\xi_1) & -\sin\theta(\xi_1)\sin\phi(\xi_1) \\ -\sin\phi(\xi_1) & 0 & \cos\phi(\xi_1) \end{bmatrix} \begin{bmatrix} \mathbf{E_1} \\ \mathbf{E_2} \\ \mathbf{E_3} \end{bmatrix} = \mathbf{W_1} \begin{bmatrix} \mathbf{E_1} \\ \mathbf{E_2} \\ \mathbf{E_3} \end{bmatrix}. \tag{3}$$

Assume that the deformed arc length coordinate is given by the parameter s. The infinitesimal length of the undeformed mid-curve $d\xi_1$ deforms to ds causing axial strain $e(\xi_1)$. If the object is subjected to shear and torsion, the orientation of the cross-section changes. The tangent vector is no longer perpendicular to the cross-section. The shearing effect is quantified by the angles $\gamma_{11}(\xi_1)$, $\frac{\pi}{2} - \gamma_{12}(\xi_1)$ and $\frac{\pi}{2} - \gamma_{13}(\xi_1)$ subtended by the directors $\mathbf{d_1}, \mathbf{d_2}$ and $\mathbf{d_3}$ with the tangent vector $\mathbf{T}(\xi_1) = \frac{\partial\boldsymbol{\varphi}}{\partial s}$. Hence, we note the following relations:

$$e = \frac{ds - d\xi_1}{d\xi_1}; \frac{\partial\xi_1}{\partial s} = \frac{1}{1+e}, \tag{4}$$

$$\boldsymbol{\varphi_{,s}} \cdot \mathbf{d_i} = \frac{1}{1+e}\boldsymbol{\varphi_{,\xi_1}} \cdot \mathbf{d_i} = \begin{cases} \cos\gamma_{1i}, \text{ when } i = 1 \\ \sin\gamma_{1i}, \text{ when } i = 2,3 \end{cases}.$$

Therefore,

$$\boldsymbol{\varphi_{,\xi_1}} = (1+e)\cos\gamma_{11}\ \mathbf{d_1} + (1+e)\sin\gamma_{12}\ \mathbf{d_2} + (1+e)\sin\gamma_{13}\ \mathbf{d_3} = (1+e)\mathbf{T}. \tag{5}$$

To define a unique relation between $\{\mathbf{T}, \mathbf{V}, \mathbf{H}\}$ and $\{\mathbf{d_i}\}$, we introduce the parameters $\alpha_1(\xi_1)$, $\alpha_2(\xi_1)$ and $\alpha_3(\xi_1)$, defined as the angles subtended by the directors $\mathbf{d_1}, \mathbf{d_2}$ and $\mathbf{d_3}$ with the vector $\mathbf{V}$ respectively. Therefore,

2

$$\begin{bmatrix} \mathbf{T}(\xi_1) \\ \mathbf{V}(\xi_1) \\ \mathbf{H}(\xi_1) \end{bmatrix} = \mathbf{W}_2 \begin{bmatrix} \mathbf{d}_1 \\ \mathbf{d}_2 \\ \mathbf{d}_3 \end{bmatrix} \tag{6}$$

The component of the orthogonal tensor $\mathbf{Q}$ in Eq. (1) can be obtained from Eq. (3) and (6) in terms of the parameters $(\theta(\xi_1), \phi(\xi_1), \gamma_{1i}(\xi_1), \alpha_i(\xi_1))$ such that $[\mathbf{Q}^\mathrm{T}]_{\mathbf{d}_i \otimes \mathbf{E}_i} = \mathbf{W}_2^{-1}\mathbf{W}_1$. The component of orthogonal matrix $\mathbf{W}_2$, the tensor $\mathbf{Q}$ and the Darboux vector can be obtained from Eq. (41), Appendix 10.1 and Appendix 10.2 respectively in Chadha and Todd [6]. Note that $\mathbf{Q}$ is orthogonal if and only if the constraints on the parameters (α_i, γ_{1i}) as mentioned in Eq. (42) of Chadha and Todd [6] are satisfied. From Eq. (2) and (5) we arrive at an important equation that governs the evolution of the system as

$$\begin{bmatrix} \boldsymbol{\varphi}_{,\xi_1} \\ \mathbf{d}_{1,\xi_1} \\ \mathbf{d}_{2,\xi_1} \\ \mathbf{d}_{3,\xi_1} \end{bmatrix} = \begin{bmatrix} 0 & (1+e)\cos\gamma_{11} & (1+e)\sin\gamma_{12} & (1+e)\sin\gamma_{13} \\ 0 & 0 & \bar{\kappa}_3 & -\bar{\kappa}_2 \\ 0 & -\bar{\kappa}_3 & 0 & \bar{\kappa}_1 \\ 0 & \bar{\kappa}_2 & -\bar{\kappa}_1 & 0 \end{bmatrix} \begin{bmatrix} \boldsymbol{\varphi} \\ \mathbf{d}_1 \\ \mathbf{d}_2 \\ \mathbf{d}_3 \end{bmatrix} \tag{7}$$

Note on the smoothness requirement of the midcurve:

Note that unique smooth curve framing by $\{\mathbf{T}, \mathbf{V}, \mathbf{H}\}$ and hence by $\{\mathbf{d}_i\}$ requires a regular C^2 curve that can have degeneracy. Thus, this frame has a relaxed condition of existence compared to the Frenet frame that needs regular C^3 non-degenerate curves.

3.   KINEMATICS OF THE BEAM-OBTAINING UNIAXIAL SCALAR STRAIN

3.1 Strain vector and deformation gradient tensor:

The position vector of any material point $\{\xi_1, \xi_2, \xi_3\}$ in the deformed configuration Ω is given by

$$\mathbf{R}(\xi_1, \xi_2, \xi_3) = \boldsymbol{\varphi}(\xi_1) + \hat{\xi}_2 \mathbf{d}_2(\xi_1) + \hat{\xi}_3 \mathbf{d}_3(\xi_1) \tag{8a}$$

where

$$\hat{\xi}_i(\xi_1, \xi_i) = (1 - e(\xi_1)v)\xi_i \text{ for } i = 2-3, \tag{8b}$$

and v represents the Poisson's ratio. Eq. (8b) represents Poisson's transformation of the cross-section. To obtain the deformation gradient tensor $\mathbf{F}$ for the problem, we define the infinitesimal tangent vector $d\mathbf{R}_0 = d\xi_1 \mathbf{E}_1$ and $d\mathbf{R}$ in Ω_0 and Ω configuration. Therefore, from Eq. (23) of Chadha and Todd [6], the tensor $\mathbf{F}$ can be obtained as,

$$\mathbf{F} = \frac{d\mathbf{R}}{d\mathbf{R}_0} = \sum_{i=1}^{3} \mathbf{R}_{,\xi_i} \otimes \mathbf{E}_i \ . \tag{9}$$

From Eq. (8), we obtain the following,

$$\frac{\partial \mathbf{R}}{\partial \xi_i} = \begin{cases} \left(\boldsymbol{\varphi}_{,\xi_1} + \hat{\xi}_2 \mathbf{d}_{2,\xi_1} + \hat{\xi}_3 \mathbf{d}_{3,\xi_1} + \hat{\xi}_{2,\xi_1} \mathbf{d}_2 + \hat{\xi}_{3,\xi_1} \mathbf{d}_3\right) & \text{when } i = 1; \\ (1 - e(\xi_1)v)\mathbf{d}_i, & \text{when } i = 2,3. \end{cases} = \boldsymbol{\lambda}_i + \mathbf{d}_i. \tag{10a}$$

where

$$\hat{\xi}_{i,\xi_1} = -e_{,\xi_1}v\xi_i \text{ for } i = 2-3. \tag{10b}$$

Using the results from Eq. (7), we obtain the expression of the vector parameter $\boldsymbol{\lambda}_i$ as

$$\boldsymbol{\lambda}_1 = \left(\left((1+e)\cos\gamma_{11} - 1\right) + \hat{\xi}_3 \bar{\kappa}_2 - \hat{\xi}_2 \bar{\kappa}_3\right)\mathbf{d}_1 + \left((1+e)\sin\gamma_{12} - \hat{\xi}_3\bar{\kappa}_1 + \hat{\xi}_{2,\xi_1}\right)\mathbf{d}_2 \tag{11}$$
$$+ \left((1+e)\sin\gamma_{13} + \hat{\xi}_{3,\xi_1} + \hat{\xi}_2\bar{\kappa}_1\right)\mathbf{d}_3;$$

3

$$\lambda_i = \left(\hat{\xi}_{2,\xi_i} - 1\right)\mathbf{d_i} = (-ve)\mathbf{d_i}, \quad \text{for i = 2 and 3.}$$

Therefore, using Eq. (8) and (9), we can obtain the deformation gradient tensor as,

$$\mathbf{F} = \sum_{i=1}^{3}(\lambda_i + \mathbf{d_i}) \otimes \mathbf{E_i} = \sum_{i=1}^{3}\lambda_i \otimes \mathbf{E_i} + \mathbf{Q}. \tag{12}$$

We define the strain vector as

$$\boldsymbol{\epsilon} = \sum_{i=1}^{3}\left(\frac{\partial \mathbf{R}}{\partial \xi_i} - \mathbf{d_i}\right) = \sum_{i=1}^{3}\lambda_i. \tag{13}$$
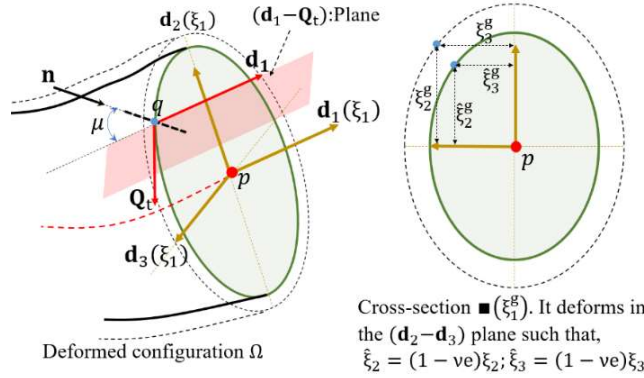
3.2 The orientation of an arbitrary strain gauge in the deformed state (measurement model):

Consider a strain gauge attached to a typical material point on the surface $q \equiv \left(\xi_2^g, \xi_3^g\right)$ on the cross-section $\blacksquare\left(\xi_1^g\right)$ in the undeformed configuration Ω_0. We assume that the strain gauge is completely attached to the material. Therefore, it maintains the angle μ with the normal vector to the cross-section. In the deformed state, the unit direction vector of the strain gauge would lie on the plane spanned the $\mathbf{d_1} - \mathbf{Q_t}$ as described in Fig. [1]. Let $\mathbf{r_{pq}} = \hat{\xi}_2^g \mathbf{d_2} + \hat{\xi}_3^g \mathbf{d_3}$ represent the vector joining the centroid of the cross-section $\blacksquare\left(\xi_1^g\right)$ to the material point q in the deformed state. The tangent vector $\mathbf{Q_t}$ for the cross-section subjected to the Poisson's contraction can be obtained as

$$\mathbf{Q_t} = \mathbf{d_1} \times \frac{\mathbf{r_{pq}}}{|\mathbf{r_{pq}}|} = -\left(\frac{\hat{\xi}_3^g}{\sqrt{\hat{\xi}_2^{g2} + \hat{\xi}_3^{g2}}}\right)\mathbf{d_2} + \left(\frac{\hat{\xi}_2^g}{\sqrt{\hat{\xi}_2^{g2} + \hat{\xi}_3^{g2}}}\right)\mathbf{d_3} = -\left(\frac{\xi_3^g}{\sqrt{\xi_2^{g2} + \xi_3^{g2}}}\right)\mathbf{d_2} + \left(\frac{\xi_2^g}{\sqrt{\xi_2^{g2} + \xi_3^{g2}}}\right)\mathbf{d_3}. \tag{14}$$

For simplicity, we assume the cross-section to be circular with the radius r in the undeformed state. Therefore, if σ is angle subtended by the vector $\mathbf{r_{pq}}$ with the vector $\mathbf{d_2}$, $\xi_2^g = r\cos\sigma$ and $\xi_3^g = r\sin\sigma$. Therefore, we obtain $\mathbf{Q_t} = -\sin\sigma\,\mathbf{d_2} + \cos\sigma\,\mathbf{d_3}$. Therefore, the unit direction vector of the strain gauge in the deformed configuration $\mathbf{n}$ is given as

$$\mathbf{n} = \cos\mu\,\mathbf{d_1} + \sin\mu\,\mathbf{Q_t} = \cos\mu\,\mathbf{d_1} - \sin\mu\sin\sigma\,\mathbf{d_2} + \sin\mu\cos\sigma\,\mathbf{d_3} \tag{15}$$

Cross-section $\blacksquare\left(\xi_1^g\right)$. It deforms in the $(\mathbf{d_2} - \mathbf{d_3})$ plane such that,
$\hat{\xi}_2 = (1 - ve)\xi_2; \hat{\xi}_3 = (1 - ve)\xi_3$

Deformed configuration Ω

Fig1: *Orientation of the strain gauge in the deformed configuration*

Notice that despite the inclusion of Poisson's effect, the unit direction vector $\mathbf{n}$ is identical to the one in Chadha and Todd [2]. This is because Poisson's effect leads to proportionate planar deformation depending on average axial strain, thereby preserving the geometric form of the cross-section.

From Eq. (11), (13) and (15), and considering $\xi_2 = \xi_2^g = r\cos\sigma$, $\xi_3 = \xi_3^g = r\sin\sigma$, $\hat{\xi}_{3,\xi_1}\left(\xi_3^g\right) = -e_{,\xi_1}v\xi_3 = -e_{,\xi_1}vr\sin\sigma$ and $\hat{\xi}_{2,\xi_1}\left(\xi_2^g\right) = -e_{,\xi_1}v\xi_2 = -e_{,\xi_1}vr\cos\sigma$, the unit scalar surface strain ϵ for the strain gauge with the unit direction vector $\mathbf{n}$ in Ω can be obtained as

$$\varepsilon = \boldsymbol{\epsilon}.\mathbf{n} = \Big[\cos\mu\Big(\big((1+e)\cos\gamma_{11}-1\big)+(1-ev)r\sin\sigma\,\bar{\kappa}_2-(1-ev)r\cos\sigma\,\bar{\kappa}_3\Big)$$
$$-\sin\mu\sin\sigma\big((1+e)\sin\gamma_{12}-(1-ev)r\sin\sigma\,\bar{\kappa}_1\big)$$
$$+\sin\mu\cos\sigma\big((1+e)\sin\gamma_{13}+(1-ev)r\cos\sigma\,\bar{\kappa}_1\big)\Big]-\sin\mu\sin\sigma\,(-ve)$$
$$+\sin\mu\cos\sigma\,(-ve) \tag{16}$$

Interestingly there is no term containing $e_{,\xi_1}$ in Eq. (16). It is not hard to prove that the expression of the surface scalar strain ε for the strain gauge on $(\mathbf{d}_1-\mathbf{Q}_t)$ plane does not have $e_{,\xi_1}$ dependence, irrespective of the shape of cross-section. Even though estimation of the parameter $e_{,\xi_1}$ is required to obtain strain vector in Eq. (13), but there is no need to estimate $e_{,\xi_1}$ for shape sensing. It is worth noting that the deformed configuration Ω of the beam can be described by $\big(\boldsymbol{\varphi}(\xi_1),\mathbf{Q}(\xi_1),e(\xi_1)\big)$ in the space $\mathbb{R}^3\times SO(3)\times\mathbb{R}$. In fact, obtaining $e_{,\xi_1}$ at a given cross-section would involve an additional strain gauge in non-tangential plane (for instance in $\mathbf{E}_2$ direction in Ω_0 configuration.)

We define the following strain parameters,

$$S_1 = (1+e)\cos\gamma_{11}-1;$$
$$S_2 = (1+e)\sin\gamma_{12};$$
$$S_3 = (1+e)\sin\gamma_{13}; \tag{17a}$$
$$S_4 = r\bar{\kappa}_1; S_5 = r\bar{\kappa}_2; S_6 = r\bar{\kappa}_3;$$

Hence,

$$e = \big((S_1+1)^2+S_2^2+S_3^2\big)^{0.5}-1 = S_7; \tag{17b}$$

Substituting Eq. (17) into Eq. (16), we arrive at the equation of surface strain in terms of parameters S_i.

4. SOLUTION APPROACH:

As mentioned in the previous section that the deformed configuration belongs to $\mathbb{R}^3\times SO(3)\times\mathbb{R}$ space, we present our solution strategy to obtain approximate configuration Ω_h that comprises of the midcurve position vector $\boldsymbol{\varphi}_h(\xi_1)$, director triad $\{\mathbf{d}_{h_i}\}$ and axial strain field $e_h(\xi_1)$. The solution to $\boldsymbol{\varphi}_h(\xi_1)$ and $\{\mathbf{d}_{h_i}\}$ is based on a localized linear basis approach, and $e_h(\xi_1)$ is estimated using moving least square approximation or equivalently, the reproducing Kernel approximation used in mesh-free methods.

4.1. An approximate solution for the midcurve position vector and director triad:

It is clear from Eq. (17) that a minimum of 6 strain gauges across the cross-section is required to determine all the deformation parameters, the same as in Chadha and Todd [2]. Unlike Chadha and Todd [2], obtaining 6 strain parameters (S_1-S_6) would involve solving a non-linear system of six simultaneous equations at a given cross-section. To obtain the approximate solution of the global deformed shape of the structure, we discretize the structure into N segments ($\bar{n}=1,\dots,N$) with the center of each segment located at $\xi_{1_{\bar{n}}}$. We attach 6 strain gauges at the right cross-section bounding the segment N at ξ_{1_n} with $n=1,\dots,N$. If we consider the left end to be fixed, the left cross-section of the first segment serves as the boundary condition. Thus, the scalar strain at the nth cross-section and for the mth strain gauge $\varepsilon_{n,m}$ can be obtained by substituting $S_i = S_{i_n}, \sigma = \sigma_{n,m}$ and $\mu = \mu_{n,m}$ in Eq. (16) and (17) as,

$$\varepsilon_{n,m} = \cos\mu_{n,m}\big(S_{1_n}+(1-S_{7_n}v)\sin\sigma\,S_{5_n}-(1-S_{7_n}v)\cos\sigma_{n,m}\,S_{6_n}\big)$$
$$-\sin\mu_{n,m}\sin\sigma_{n,m}\big(S_{2_n}-(1-S_{7_n}v)\sin\sigma_{n,m}\,S_{4_n}-vS_{7_n}\big) \tag{18}$$
$$+\sin\mu_{n,m}\cos\sigma_{n,m}\big(S_{3_n}+(1-S_{7_n}v)\cos\sigma_{n,m}\,S_{4_n}-vS_{7_n}\big)$$

Here, $\sigma_{n,m}$ is the angle subtended by the mth strain gauge with the normal vector $\mathbf{d}_1$ on the cross-section of the nth cross-section and S_{7_n} depends on other strain terms as per Eq. (17b). Note that unlike the definition of the deformed configuration of the beam in Chadha and Todd [2], here the cross-section also undergoes Poisson's transformation. Therefore, it is necessary to determine the approximate axial strain $e(\xi_1)$ along with the midcurve position vector $\boldsymbol{\varphi}(\xi_1)$ and the director triad $\{\mathbf{d}_i\}$. For the nth cross-section, the discrete differential equations governing the configuration Ω is same as Eq. (18) of Chadha and Todd [2].

We use local linearization approach where the coefficients in the governing differential equation are linearized locally in each segment. We tractate a Taylor series expansion of the seven coefficients about the location of the cross-section $\xi_1 = \xi_{1_n}$ to

zeroth order, thereby reducing the system of differential equations (7) into a constant-coefficient system that admits exact solution, valid locally at each segment. The solution for the nth segment is,

$$\boldsymbol{\varphi_n}(\xi_1) = \mathbf{A_{n_1}}\xi_1 + \mathbf{A_{n_2}} \sin\left(\frac{\xi_1\gamma_n}{r}\right) + \mathbf{A_{n_3}} \cos\left(\frac{\xi_1\gamma_n}{r}\right) + \mathbf{A_{n_4}} \tag{19a}$$

$$\mathbf{d_{n_i}}(\xi_1) = \mathbf{B_{n_{i_1}}}\xi_1 + \mathbf{B_{n_{i_2}}} \sin\left(\frac{\xi_1\gamma_n}{r}\right) + \mathbf{B_{n_{i_3}}} \cos\left(\frac{\xi_1\gamma_n}{r}\right) + \mathbf{B_{n_{i_4}}}, \text{ where } \gamma_n = \left(\sum_{i=4}^{6} S_{i_n}^2\right)^{\frac{1}{2}} \tag{19b}$$

The vector constants $\mathbf{A_{n_1}} - \mathbf{A_{n_4}}$ in Eq. (21a) can be found as described in Appendix (A.2) of Chadha and Todd [2]. In fact, these vector constants ($\mathbf{A_{n_1}} - \mathbf{A_{n_4}}$ and $\mathbf{B_{n_{i_1}}} - \mathbf{B_{n_{i_4}}}$) are function of the strain parameters $S_{1_n} - S_{6_n}$ and the constants of integration. Hence, if there are N cross-sections, there are 12N constants of integration. Imposing continuity in each component of $\{\boldsymbol{\varphi_n}, \mathbf{d_1}, \mathbf{d_2}, \mathbf{d_3}\}$ between the segments gives $12(N-1)$ constraints, and an appropriate boundary condition gives 12 additional conditions. The estimated value of the axial strain at the cross-section location can be obtained from Eq. (17b). If all the strain parameters S_{i_n} are zero (implying a point of degeneracy), then Eq. (20) of Chadha and Todd [2] guarantees that the solution basis has no singularity. The global approximate solution for $\boldsymbol{\varphi_h}(\xi_1)$ and $\{\mathbf{d_{h_i}}\}$ can be obtained by stitching together each of these local solutions using the Heaviside function as in Eq. (21) of Todd et al [1].

4.2. Approximate solution to the axial strain

Equation (17b) can be used to obtain the axial strain $e(\xi_{1_n})$ in the nth cross-section. We approximate the axial strain field using Moving Least square approximation. We brief the approach here. Let $\mathbf{P}(\xi_1) = \{1, \xi_1, \xi_1^2, \dots, \xi_1^m\}^T$ represent set of mth order polynomial basis set, ξ_{1_n} represent n^{th} location of discrete cross-section and $W(\xi_1 - \xi_{1_n})$ represent the moving weight function, then the approximate axial strain and curvature field is given as,

$$e_h(\xi_1) = \mathbf{P^T}(\xi_1)\mathbf{M}^{-1} \sum_{n=1}^{N} \mathbf{P}(\xi_{1_n})e(\xi_{1_n})W(\xi_1 - \xi_{1_n}) \tag{20a}$$

Where,

$$\mathbf{M} = \text{Moment matrix} = \sum_{n=1}^{N} \mathbf{P}(\xi_{1_n})\mathbf{P^T}(\xi_{1_n})W(\xi_1 - \xi_{1_n}); \tag{20b}$$

$$e(\xi_{1_n}) = \left((S_{1_n} + 1)^2 + S_{2_n}^2 + S_{3_n}^2\right)^{0.5} - 1; \tag{20c}$$
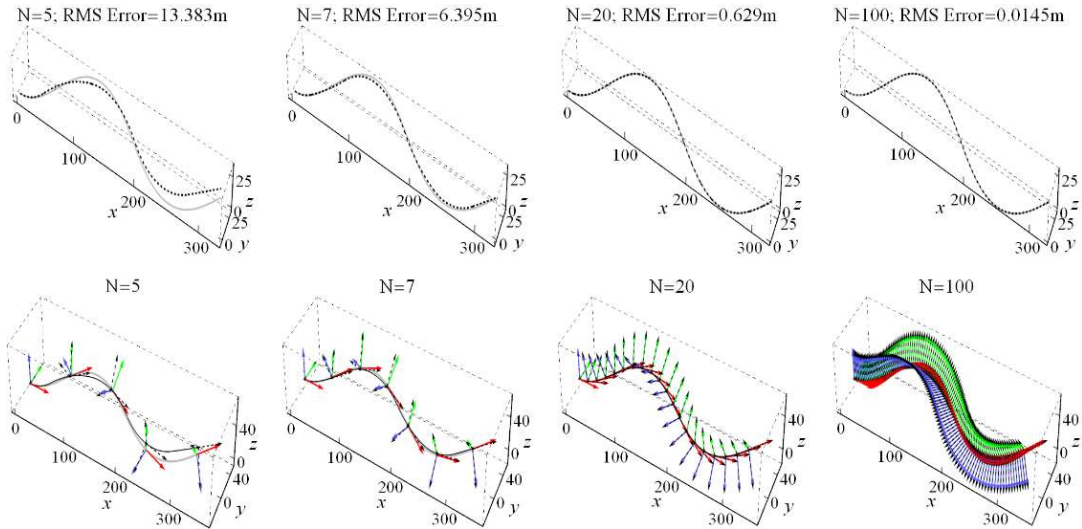
One of the most commonly used weight function is cubic B spline, such that

$$W(\xi_1 - \xi_{1_n}) = W(z_n) = \begin{cases} \frac{2}{3} - 4z_n^2 + 4z_n^3, & \text{for } 0 \le z_n \le 0.5 \\ \frac{4}{3} - 4z_n + 4z_n^2 - \frac{4}{3}z_n^3, & \text{for } 0.5 \le z_n \le 1 \\ 0 & \text{otherwise} \end{cases}; \ z_n = \frac{|\xi_1 - \xi_{1_n}|}{a} \tag{21}$$

The term a is the support size. For m^{th} order basis set, the weight function must be spread enough to cover at least $(m + 1)$ data points. This fact is used to evaluate the support size. In a similar fashion, the approximate curvature fields $\bar{\kappa}_{h_1}, \bar{\kappa}_{h_2}$ and $\bar{\kappa}_{h_3}$ can be obtained.

5. SIMULATION:

We simulate a 300m long circular rod with $\nu = 0.3$ and diameter of 30.48 cm to study the effect of multiple curvatures, axial strain, Poisson's deformation, but no shear. Unlike Chadha and Todd [2] the shape sensing now depends on the material property ν. The strain value at the surface of Ω for assumed orientation of strain gauge was obtained using Eq. (16). The strain parameters for the given cross-section were obtained by solving the non-linear simultaneous equations in Eq. (18). The approximate configuration Ω_h is obtained using Eq. (19a-19b) and Eq. (20a). The assumed midcurve shape bears two points of degeneracy. The algorithm is thus without any singularity. We assume the orientation of the surface strain gauges given by $\sigma_n = \left\{\frac{\pi}{4}, \frac{\pi}{2}, \frac{3\pi}{4}, \pi, \frac{5\pi}{4}, \frac{3\pi}{2}\right\}$ and $\mu_n = \left\{\frac{\pi}{4}, -\frac{\pi}{4}, \frac{\pi}{4}, -\frac{\pi}{4}, \frac{\pi}{4}, -\frac{\pi}{4}\right\}$.

Fig2: *Top plots: Comparison of exact midcurve* $\varphi(\xi_1)$ *(light gray solid line) and the reconstructed approximate midcurve* $\varphi_h(\xi_1)$ *(dashed line). Bottom Plots: Comparison of exact directors (*d_1, d_2 *and* d_3 *are represented by red, green and blue vectors respectively) and the predicted directors (*$\{d_{h_i}\}$ *represented by black-dashed directors) of the object.*
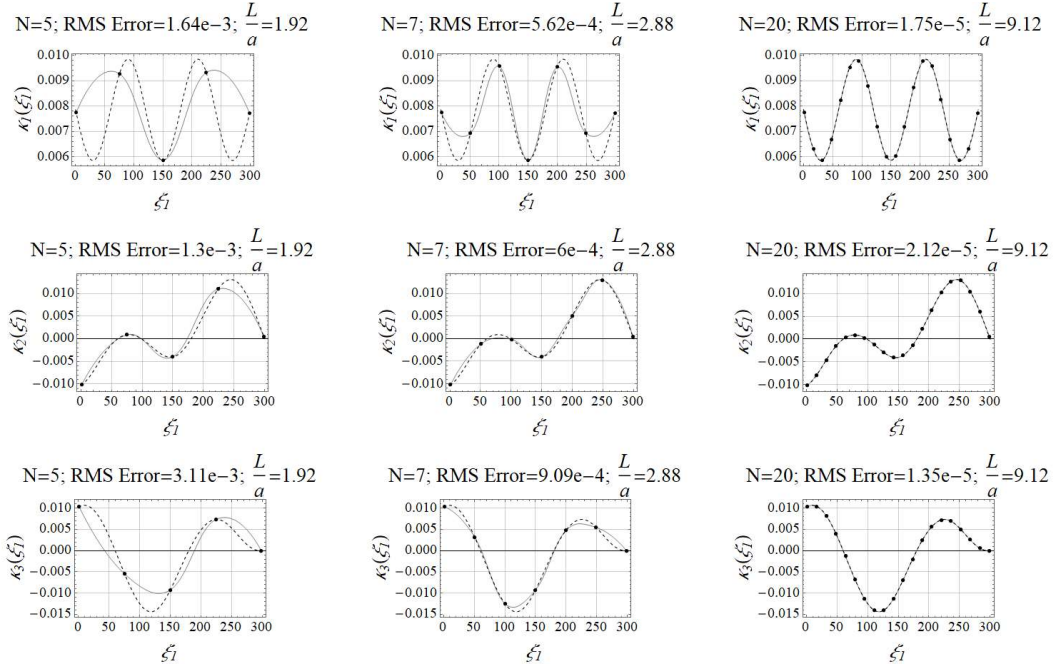
Fig3: *Comparison of exact curvature terms* $\kappa_i(\xi_1)$ *(dashed line) and the approximate axial strain* $\kappa_{i_h}(\xi_1)$ *(light gray solid line). The dots represent the data points obtained from the surface strain values.*
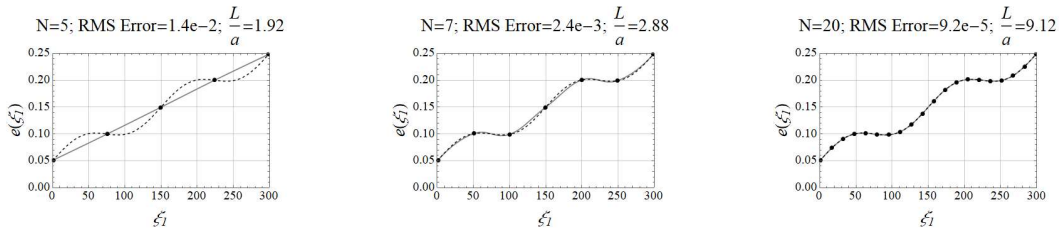
Fig4: *Comparison of exact axial strain* $e(\xi_1)$ *(dashed line) and the approximate axial strain* $e_h(\xi_1)$ *(light gray solid line). The dots represent the data points obtained from the surface strain values and used for global approximation.*

7

Figure [2] compares the exact midcurve $\boldsymbol{\varphi}(\xi_1)$ with the approximate midcurve $\boldsymbol{\varphi}_h(\xi_1)$ and the exact orientation field $\{\mathbf{d}_i\}$ with the approximate field $\{\mathbf{d}_{h_i}\}$, solved using linearized analytical inverse approach for 5, 7, 20 and 50 discretized cross-sections. The RMS Error is mentioned on top of the plots. The RMS Error reduces exponentially with the increase in number of cross-section at which strain gauge is attached.

Figure [3] and [4] compares the exact curvature and axial strain field with the approximated fields. The approximation is obtained using Moving Least Square approximation. In this simulation, we use 2nd order shape function. The parameter $\frac{L}{a}$ in Fig. [3] and [4] represents the ratio of the undeformed length of beam and the support size chosen for the approximation. Therefore, the approximation algorithms suggested in section 4 gives an excellent (as well as converging) reconstruction of the deformed configuration.

As explained in Chadha and Todd [2], there are three main sources of error: uncertainty in the boundary condition, noise in the strain measurements, and error due to approximation.

6. CONCLUSION:

In this paper, we improve the theory of shape sensing by incorporating Poisson's effect, thereby partially relaxing Euler-Bernoulli's rigid cross-section assumption such that the cross-section could undergo planar Poisson's transformation. The problem still maintains its single manifold nature where the configuration of the structure is defined by the mid-curve, director triad, and the axial strain, all being function of the undeformed arclength ξ_1. Unlike Chadha and Todd [2] where the configuration was defined in $\mathbb{R}^3 \times SO(3)$ space, here the configuration is defined in $\mathbb{R}^3 \times SO(3) \times \mathbb{R}$ space.

We briefly defined the finite strain parameters, obtained expression for deformation gradient tensor and strain vector. Unlike [1-2] the second and third component of an infinitesimal vector in the undeformed state are also strained due to Poisson's effect. Another observation is that the unit direction vector bears the same expression as in [2]. This is because Poisson's transformation does not change the form of the cross-section. For instance, ellipse remains ellipse Poisson's transformation except for different major and minor axis. The ratio of major to minor axis lengths remains the same.

The number of strain gauges per cross-section remains the same as in [2] but obtaining $(S_1 - S_6)$ from the scalar surface strain measurements now involves solving for 6 nonlinear simultaneous equations. The global solution to the set of differential equations obtained is determined using the continuity conditions and boundary conditions. The axial strain and the curvature fields can be estimated by a moving least squares continuous approximation. The suggested reconstruction strategy is convergent and non-singular even if the midcurve has multiple points or segment of degeneracy. The RMS error reduces exponentially with the increase in number of cross-sections.

REFERENCES:

[1]. Todd, M. D., Skull, C. J., and Dickerson, M., 2013, "A local material basis solution approach to reconstructing the three-dimensional displacement of rod-like structure from strain measurements," ASME Journal of Applied Mechanics, 80(4), DOI: 10.1115/1.4023023.

[2]. Chadha, M., Todd, M. D., 2017, "A generalized approach to reconstructing the three-dimensional shape of slender structures including the effects of curvature, shear, torsion, and elongation," ASME Journal of Applied Mechanics, DOI:10.1115/1.4035785.

[3]. Chadha, M., Todd, M.D., 2018, "A Displacement Reconstruction Strategy for Long, Slender Structures from Limited Strain Measurements and Its Application to Underground Pipeline Monitoring." In: Conte J., Astroza R., Benzoni G., Feltrin G., Loh K., Moaveni B. (eds) Experimental Vibration Analysis for Civil Structures. EVACES 2017. Lecture Notes in Civil Engineering, vol 5, pp. 317-327 Springer, Cham

[4]. Cosserat, E., and Cosserat, F., 1909, *Theorie des Corps Deformable*, Herman, Paris, France.

[5]. Ericksen, J. L., and Truesdell, C., 1958, "Exact theory of stress and strain in rods and shell", Arch. Rational Mech. Analysis, 1, pp.295-323.

[6]. Chadha, M., Todd, M. D., 2017, "An introductory treatise on reduced balance laws of Cosserat beams," International Journal of Solids and Structures, 126-127, pp.54-73.